

The influence of Coulomb interaction of localized charges on low-temperature scanning tunnelling spectra of surface nanodefects

This article has been downloaded from IOPscience. Please scroll down to see the full text article.

2001 J. Phys.: Condens. Matter 13 3941

(<http://iopscience.iop.org/0953-8984/13/18/304>)

View [the table of contents for this issue](#), or go to the [journal homepage](#) for more

Download details:

IP Address: 171.66.16.226

The article was downloaded on 16/05/2010 at 11:54

Please note that [terms and conditions apply](#).

The influence of Coulomb interaction of localized charges on low-temperature scanning tunnelling spectra of surface nanodefects

N S Maslova^{1,3}, A I Oreshkin¹, S I Oreshkin¹, V I Panov¹, S V Savinov¹
and A A Kalachev²

¹ Moscow State University, Department of Physics, 119899 Moscow, Russia

² Institute of Physics, Humbolt University, Berlin, Germany

E-mail: spm@spmlab.phys.msu.su (N S Maslova)

Received 20 November 2000, in final form 7 March 2001

Abstract

In the present work we report experimental and theoretical results of investigations of the local electronic properties of highly oriented pyrolytic graphite (HOPG) over a wide temperature range by means of a scanning tunnelling microscope (STM)/scanning tunnelling spectroscopy technique. We have examined artificial nanodefects produced by remote plasma treatment on a (0001) HOPG surface. We have found substantial differences between STM topographic images as well as between local spectroscopy data measured at room temperature and at He temperatures. We believe that this difference is caused by the strong decrease of the relaxation rate of non-equilibrium electrons in STM junctions at lower temperatures resulting in the appearance of localized charges in the contact area.

1. Introduction

Graphite is known as one of the subjects most widely chosen for investigation in STM/STS experiments from the very beginning because it is a simple mono-component layered crystal, suitable both for experimental and for theoretical investigation. Its layered structure provides the possibility of obtaining large inert atomically flat areas by simple mechanical cleaving. But some anomalous features have long been observed experimentally, such as giant atomic corrugation height and different long-range electron-density structures superimposed on the graphite lattice above flat surface areas and near surface defects [1–4]. The quasi-two-dimensional structure of graphite monolayers and the interaction with adjacent layers make surface carbon atoms non-equivalent, which might explain why only three of the six atoms forming the carbon hexagon are visible in STM images. This asymmetry should become less pronounced or even disappear in the case of graphite intercalation compounds, where

³ Author to whom any correspondence should be addressed.

intercalation increases the distance between neighbouring layers and changes the charge distribution, so interlayer interaction can be neglected [5, 6].

It is also well known that surface defects of different kinds (metallic clusters, atomic vacancies, surface layer dislocations etc) are surrounded by $(\sqrt{3} \times \sqrt{3})R30^\circ$ charge structures which disappear a few nanometres away from the defect [5]. At the same time, charge structures with sixfold symmetry and periodicity up to 7 nm were observed even above flat graphite surfaces. The existence of various superstructures has often been explained as arising from the interference of scattered electron wave functions with energies lying near the Fermi level and by a quasi-two-dimensional structure of the graphite lattice [3].

All of these effects are connected with charge redistribution in a few graphite (sub)surface layers. The properties of perfect graphite monolayers (even without defects of any kind) are strongly influenced by electron–electron interaction. Non-uniform charge distribution (such as charge-density waves) on the surface can appear if the on-site Coulomb interaction and repulsive interaction of charges occupying adjacent sites are taken into account. In the presence of nanoscale defects and/or a STM tip, the Coulomb interaction of localized charges starts to play a more significant role and strongly modify the local electronic density of states [7, 8].

In the present work we report experimental and theoretical results of investigations of the local electronic properties of HOPG over a wide temperature range by means of a STM/STS technique. We have examined artificial nanodefects produced by remote plasma treatment on (0001) HOPG surfaces [9]. In general, there is great interest in the study of surface structures (including artificially produced defects of different kinds) having sizes of a few nanometres. Our experiments were carried out both at room temperature and at low temperature (LT): 4.2 K. We have found substantial differences between STM topographic images as well as between the local spectroscopy data. We believe that this difference is caused by the strong decrease of the relaxation rate of non-equilibrium electrons in STM junctions on lowering the temperature. The relaxation rate due to electron–phonon interaction has been estimated to be of the order of 10^8 s^{-1} for temperature of about 1 K [10, 11]. This relaxation rate is smaller than the tunnelling rate, which is of the order of 10^9 – 10^{10} s^{-1} for current values of 10–100 pA.

Artificial nanodefects on graphite surfaces can be treated as tunable Anderson impurities, similarly to quantum dots on semiconductors. Experimental STM/STS investigations of such objects reveal a crucial role of the Coulomb interaction, and relaxation processes resulting in non-equilibrium character of the local tunnelling conductivity. The STM tip apex can also act as an ultrasmall metallic quantum dot in the non-equilibrium state. At finite values of applied bias, the Coulomb interaction energy is sensitive to the occupation configuration of tip-localized states and can vary due to non-equilibrium fluctuations of electron filling numbers. Thus, fluctuations in scanning tunnelling spectra can also be observed in the non-equilibrium case. So, we suggest that low-temperature tunnelling conductivity spectra of nanodefects reflect non-equilibrium charge distribution in the contact area leading to changes in energy of the tip- or defect-localized states.

2. Experimental results and discussion

The procedure of production of artificial defects on the HOPG surface is described elsewhere [9]. The resulting nanopits are mainly one monolayer in depth. The characteristic lateral size and the distance between neighbouring defects depend on the fabrication procedure. We have investigated HOPG samples with nanopit sizes in the range from 1 nm to 30 nm. Summarizing the results of the room temperature investigations, we can state the following [12]. According to our measurements, nanopits look like craters with bumps at the edges and have rectangular shape rather than being round. We did not observe any additional surface

structure superimposed on the HOPG lattice around the defects. Tunnelling spectroscopy curves acquired above flat surface areas did not reveal any specific features. At the same time we found well pronounced peaks separated by a 100–200 meV gap in the tunnelling conductivity curves measured above nanofeatures 1–10 nm in size. As the defect size becomes larger the gap between the peaks decreases, and finally for nanopits greater than 15 nm additional structure in the tunnelling spectra completely vanishes. We connect the observed behaviour of the tunnelling conductivity with the existence of dimensional quantization levels (DQL) localized near the defect [12]. For two nanopits where DQL exist which are located close enough to each other, DQL split into two. This situation was observed for two 3 nm nanopits situated 2 nm apart. Instead of each single peak we obtained a double peak split by approximately 40 meV (figure 1).

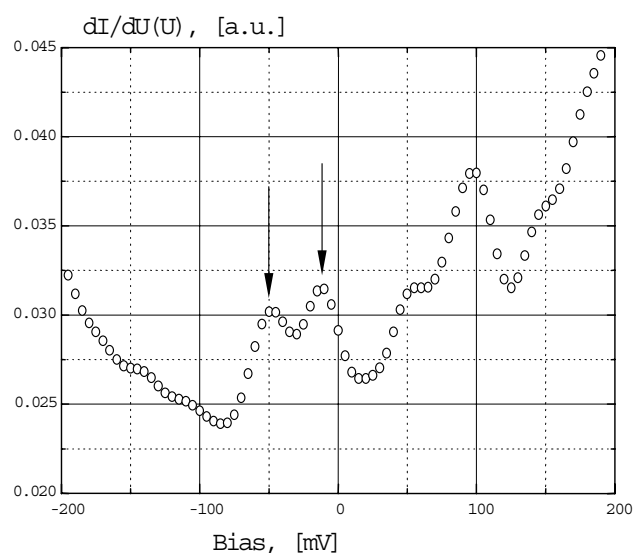


Figure 1. Tunnelling conductivity curves, measured at room temperature above a nanopit with another nanopit in the near (distance of the order of the diameter, ~ 0.1 nm) neighbourhood.

In the LT STM experiments we used the same samples as were investigated at room temperature. Details of the experimental set-up were described elsewhere [13]. At helium temperature, the thermal broadening is smaller by two orders of magnitude than that at room temperature. So, at first glance one would expect the peak structure in the tunnelling conductivity caused by dimensional quantization effects to be more evident at low temperature. But our STM/STS observations are at variance with this simplified point of view. We have obtained tunnelling conductivity spectra which are obviously different from the room temperature spectra. A few peaks in the tunnelling spectra are clearly seen both above nanopits and above flat surface areas as far as 50 nm away from the defect. The distance between neighbouring peaks is approximately 500 meV, which strongly exceeds the spacing between DQL observed at room temperature.

Besides this, in STM images we have observed additional structure superimposed on the HOPG lattice around isolated nanopits. It corresponds approximately to the well known $(\sqrt{3} \times \sqrt{3})R30^\circ$ structure [3, 5]; it decays with the distance from the defect and finally disappears 20 nm away from the nanopit (figure 2). If two defects are situated closer than this characteristic decay length, one can observe the superposition of additional structures between defects. Similar STM topography was reported in [6]. The authors investigated nanopits

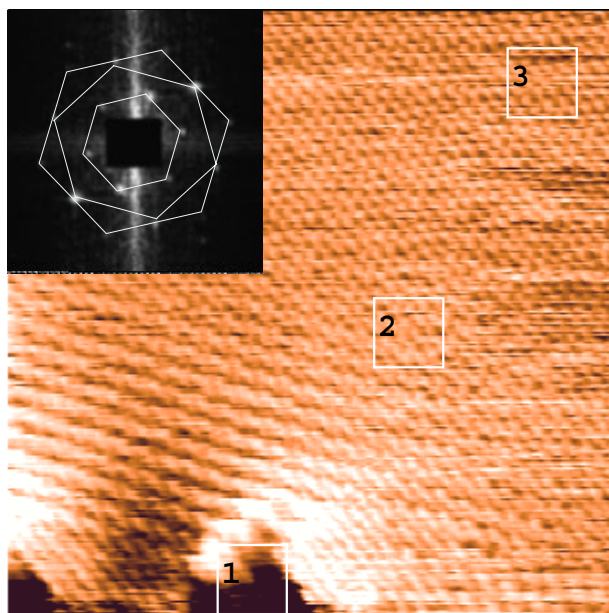


Figure 2. An STM image of a (0001) surface of HOPG near a defect one monolayer in depth at low temperature. The apparent charge structure is superimposed on the HOPG atomic lattice. The inset depicts the Fourier transform of the image, illustrating that doubled frequency as well as a $(\sqrt{3} \times \sqrt{3})R30^\circ$ superstructure are present at the surface.

(This figure is in colour only in the electronic version, see www.iop.org)

created *in situ* on HOPG surfaces under UHV conditions both at room temperature and at low temperature. They did not observe any superstructures at room temperature; however, well pronounced structures were reported for low temperature.

We ascribe the different results of the STM investigations at low temperature to the prevailing role of charge effects at low temperature. This is surprisingly consistent with the idea that superstructures on HOPG surfaces are analogous to Friedel oscillations [14].

In the general case, in the vicinity of defects of any kind, the local density of states (LDOS) is modified compared to the LDOS of the unperturbed surface. But the possibility of experimental STM observation of different features in the LDOS depends on the following factors: the STM tip electronic structure, the tip-sample interaction and the relaxation rate of the non-equilibrium electrons. Usually the STM tip is treated as ideal metal with a smooth LDOS. In a more realistic treatment there should be localized states at the STM tip connected with the edge cluster of atoms at the tip apex. Tip-sample interaction and a finite relaxation rate can lead to a non-equilibrium electron distribution in the STM contact area resulting in additional charges being localized on the STM tip apex or near the defect [7].

The energy value of the DQL can be estimated simply [12], but quantitative analysis requires knowledge of the exact geometry of the potential, which is connected with the defect and is not well defined in the case of a thermally etched HOPG surface. A geometrical dip causes a local rise in potential for electrons, while a geometrical bump creates a potential well. At the same time, the shape of the effective potential does not coincide with the geometrical shape of the defect. There is only a qualitative correlation. With the increase of the defect lateral size, the effective radius of the potential also becomes larger and the distance between the DQL decreases [12]. If the effective potential width/depth is too wide/small or it is strongly

asymmetric, there will be no bound states in this potential [15]. Thus we did not observe DQL for nanopits greater than 15 nm in diameter. Another reason is that the thermal broadening (25 meV at room temperature) is comparable with the spacing between the DQL when the DQL cannot be resolved. Tip-sample interaction causes strong renormalization of the initial electronic spectrum and is especially important for systems with reduced dimensionality [8]. The energy of the tip states depends on the value of the non-equilibrium charges. In the initial stage, the charge becomes larger with increasing applied bias voltage or tunnelling current. But then saturation occurs, because the filling number of a certain localized state for an electron with a particular spin cannot exceed one, due to the Fermi statistics. The dependence of the non-equilibrium charge on the applied bias for impurities on semiconductor surfaces was analysed in [7]. As the charge accumulated in a localized state is determined by the relaxation and tunnelling rates, it also depends on the tip-sample and tip-defect separations. By changing the STM tip position one can obtain various tunnelling conductivity curves with different peak positions. Finally, at room temperature one can observe DQL with energy spacing Δ_1 if localized states connected with the tip apex reside far below the Fermi level, as is shown in figure 3(a). Also there are no localized charges that can shift the energy levels of these states due to the Coulomb interaction. In this case, tip-localized states do not influence the tunnelling current. At low temperature, in contrast, tip states start to play an important role in tunnelling processes. A smaller relaxation rate can lead to non-equilibrium electron distribution in the contact area, resulting in the appearance of localized charges at the tip apex [7]. On-site Hubbard-type interaction of localized charges shifts the initial energy levels of the tip states toward the Fermi level. Also, the energy of the localized state now depends on the electron filling numbers. So, a single spin-degenerate localized tip state can lead to the presence of a

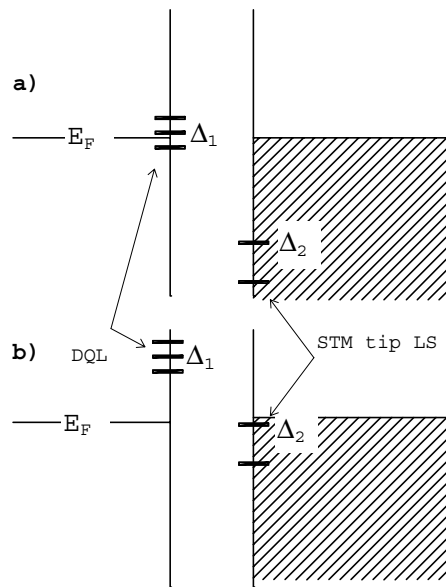


Figure 3. A schematic diagram of the Coulomb shift of the sample DQL and tip-localized states. Δ_1 : the energy spacing between the sample DQL; Δ_2 : the energy spacing of the tip-localized states. (a) Localized charges are absent. The tip-localized states are located far below the Fermi energy. This situation is usual for room temperature. (b) At low temperature, the on-site Coulomb repulsion changes the energies of the localized states. The tip states are now near the Fermi level and the DQL are shifted away.

pair of peaks in an experimental tunnelling conductivity curve due to the Coulomb interaction. Such peaks are separated by an energy gap which has an energy value typical for Coulomb repulsion at the 1 nm scale: about 0.5–1 eV [16]. A charged tip also changes the initial electron spectrum of the sample surface. Coulomb interaction of localized tip charges with sample electrons shifts the DQL away from their initial position near the Fermi level (up/down depending on the sign of the tip charge: negative/positive). The characteristic value for this shift is also about 0.5–1 eV. The modification of the effective electron spectrum near the defect caused by the Coulomb interaction with the tip charge is roughly illustrated in figure 4. Here we restrict the consideration to just the shift of the initial existing DQL. The energies of the DQL are also sensitive to the filling numbers of the electrons localized on the defects. Changes in electron filling numbers also shift the DQL (up/down) as in the Coulomb-blockade regime. The determination of the electron spectrum near the defect in the presence of Coulomb interaction requires a self-consistent approach, taking into account non-equilibrium kinetic processes [7].

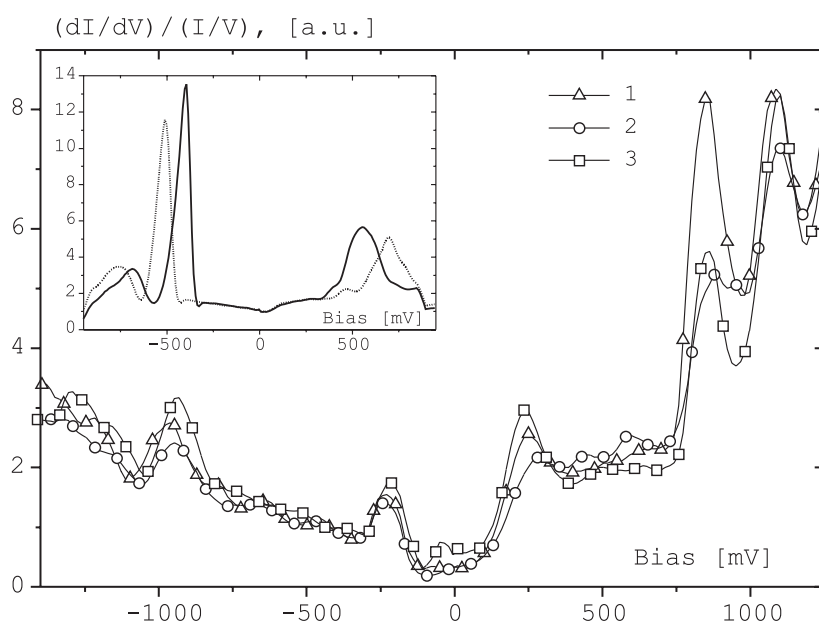


Figure 4. A set of tunnelling conductivity curves, measured in the vicinity of a nanod defect. The curves are averaged within the areas shown in figure 2 and then numerically differentiated. One can see a slight dependence of the peaks at -1 V, -0.25 V and $+0.25$ V on the distance from the defect. The peaks around $+1$ V change quite noticeably. The inset shows tunnelling spectra measured above a flat area far from any defects at two spots separated by 20 nm. The peaks can be attributed to the influence of the states localized at the STM tip apex.

Thus, we believe that in low-temperature experiments the tunnelling conductivity near the Fermi level is determined by the charged tip states, whose energy depends on the electron filling numbers, and not by the DQL. Schematically, this situation is depicted in figure 3(b). It is obvious that if the DQL are shifted away from the Fermi level, they will not contribute to the tunnelling current. The tunnelling conductivity curves for the flat surface region should be similar to those for near the defect, and they are determined by the electron spectrum of the charged tip. Anomalies in tunnelling conductivity spectra have now been connected with the tip-localized energy spacing Δ_2 and the value of the Coulomb interaction of the localized charges. Our experimental data confirm this suggestion. A set of peaks separated

by approximately 0.5 eV are present in the tunnelling conductivity curves. The positions of the peaks are constant and their heights change only slightly with distance from the nanopit (figure 4).

Further clear evidence of the Coulomb interaction of localized charges is provided by the very strong modification of the initial sample's electronic spectrum during STM measurements. Huge peaks can be seen in the voltage ranges where specific features of the initial sample's LDOS lead to the most rapid growth of the tunnelling current with the tunnelling bias, resulting in strong self-consistent changes of the localized charge. The overall shape of the tunnelling spectra can be drastically changed (see the inset to figure 4). Similar charge effects were observed on semiconductor surfaces [16]. Self-consistent theoretical analysis of the influence of the Coulomb interaction of localized charges explained the strong changes of the STS-measured tunnelling conductivity as compared to the density of states of the unperturbed sample, and it also predicted the appearance of tunnelling conductivity (TC) peaks near fundamental bandgap edges [7].

Because of the preparation procedure, nanopits are randomly distributed on the surface. At LT and rather high defect concentration, one can expect tunnelling conductivity anomalies caused by weak localization. But it is difficult to observe these anomalies in scanning tunnelling spectra because the localization radius is greater than the mean free path—i.e. the mean distance between the defects.

3. Conclusions

In the present work we report experimental and theoretical results of investigations of the local electronic properties of HOPG over a wide temperature range by means of a STM/STS technique. We have examined artificial nanodeflects produced by remote plasma treatment on (0001) HOPG surfaces. We have found substantial differences between STM topographic images as well as between local spectroscopy data. We believe that this difference is caused by a strong decrease of the relaxation rate of the non-equilibrium electrons in the STM junction at low temperature and the appearance of interacting localized charges in the contact area. Coulomb interaction of such non-equilibrium charges strongly modifies the initial spectrum of the localized states and the tunnelling conductivity spectra obtained experimentally.

Acknowledgments

This work was financially supported by the Russian Ministry of Research (Surface Atomic Structures, grant 1.22.99; Micro- and Nanoelectronic, project 5.2.40.E49) and the Russian Foundation of Basic Research (RFBR, grants 00-02-17759, 00-15-96555).

References

- [1] Mochiji K, Yamamoto S, Shimutzu H, Ohtani S, Seguchi T and Kobayashi N 1997 *J. Appl. Phys.* **82** 6037
- [2] Vandervoort K G, MacLain K N and Butcher D J 1997 *Appl. Spectrosc.* **51** 1896
- [3] Klusek Z, Kalinowski M W, Oleniczak W and Kobierski P 1997 *Proc. 1st Int. Symp on SPM and Related Methods (Poznan)* p 415
- [4] Kappel M, Steidl M, Biener J and Kupperts J 1997 *Surf. Sci.* **387** L1062
- [5] Takeuchi N, Valenzuela-Benavides J and Marales de la Garsia L 1997 *Surf. Sci.* **380** 190
- [6] Hovel H, Becker Th, Bettac A, Reihl B, Tschudy M and Williams E J 1997 *J. Appl. Phys.* **81** 154
- [7] Arseyev P I, Maslova N S and Savinov S V 1998 *JETP Lett.* **68** 320
- [8] Arseyev P I and Maslova N S 1992 *Sov. Phys.-JETP* **75** 575
- [9] Tracz A, Kalachev A A, Wegner G and Rabe J P 1995 *Langmuir* **11** 2840

-
- [10] Agam O, Wingreen N and Altshuler B L 1997 *Phys. Rev. Lett.* **78** 1956
 - [11] Depuydt A *et al* 1999 *Phys. Rev. B* **60** 2619
 - [12] Maslova N S, Oreshkin A I, Panov V I, Savinov S V, Kalachev A A and Rabe J P 1995 *Solid State Commun.* **95** 507
 - [13] Oreshkin S I, Panov V I, Savinov S V, Vasilev S I, Depuydt A and Van Haesendonck C 1997 *Prib. Tekh. Eksp.* **4** 145
 - [14] Mizes H A and Foster J S 1989 *Science* **244** 559
 - [15] Landau L D and Lifshitz I M 1989 *Quantum Mechanics* 4th edn (Moscow: Nauka) p 768
 - [16] Maslova N S, Panov V I, Savinov S V, Depuydt A and Van Haesendonck C 1998 *JETP Lett* **67** 147